Magnetic properties of a quasi-two-dimensional Heisenberg antiferromagnet α-$RbCrF_4$

Yoko Miura[1*] and Ryota Sueyoshi[2], Hirotaka Manaka[2]

[1]National Institute of Technology, Suzuka College, Shiroko-cho, Suzuka, Mie 510-0294, Japan
[2]Graduate School of Science and Engineering, Kagoshima University, Korimoto, Kagoshima 890-0065, Japan

.

ABSTRACT

We synthesized a quasi-two-dimensional Heisenberg antiferromagnet on a square lattice formed in α-$RbCrF_4$ by improving the pretreatment method before primary sintering. From X-ray diffraction measurements, the crystal structure was found to consist of a $TlAlF_4$-type structure, which shows a good two-dimensionality. Temperature dependence of magnetic susceptibility shows a broad peak, which indicates typical low-dimensional antiferromagnets, at $T_{\mathrm{max}} \approx 47\ \mathrm{K}$. Furthermore, a sharp peak which indicates an antiferromagnetic phase transition also appeared at T_N = 29.3(2) K. Following several previous theoretical investigations, we estimated intra-layer (J_{intra}) and inter-layer (J_{inter}) exchange interactions to be $J_{\mathrm{intra}} / k_{\mathrm{B}} = -6.6(1)\ \mathrm{K}$ and $J_{\mathrm{inter}} / J_{\mathrm{intra}} \approx 0.05$, respectively. As a result, we found that α-$RbCrF_4$ is a quasi-two-dimensional Heisenberg antiferromagnet.

Keywords: Quasi-two-dimensional magnet, X-ray diffraction, magnetic susceptibility, α-$RbCrF_4$

1. INTRODUCTION

Recently, magnetoelectric multiferroic materials have received much attention because of the possibility of either "magnetic control of ferroelectric domains" or "electric control of magnetic domains"[1,2,3]. In ferromagnetics and ferroelectrics, the switching from one domain orientation to another occurs because of the application of external perturbation, which changes the preferred, lowest energy orientation of the order parameter from one state to another. In addition to magnetic and electric fields, mechanical stress can have a switching effect in ferroelastic materials. In addition to magnetic and electric fields, mechanical stress can have a switching effect in ferroelastic materials. Using point groups of prototypic and ferroic phases, Aizu classified the cases where ferromagneticity, ferroelectricity, and ferroelasticity coexist and completely couple with each other[4].

Many investigations have been reported for successive structural phase transitions in $A^{\mathrm{I}}M^{\mathrm{III}}F_4$ compounds, where the $M^{\mathrm{III}}F_6$ octahedra are centered in a square-based parallelepiped of A^+ cations in the so-called $TlAlF_4$-type structure[5]. Figure 1 shows an aristotype $A^{I}M^{III}F_4$ structure. The corner-sharing $M^{III}F_6$ octahedra result in a square lattice with each layer separated by A^{I} cations, leading to a good two-dimensionality in $A^{I}M^{III}F_4$ compounds. For example, in non-magnetic compounds $TlAlF_4$ and $RbAlF_4$[6,7], internal strains were investigated and the switching of ferroelastic domains by uniaxial stress was demonstrated, although a ferroelastic-ferroelectric effect can not be expected because of the non-polar space group of these materials. Furthermore, in magnetic compounds with S = 5/2, $RbFeF_4$ and $CsFeF_4$[8,9,10,11], an orthorhombic (mmm)-tetragonal (4/mmm) structural phase transition causes spontaneous strain, and then, an antiferromagnetic phase transition occurs far below the structural phase transition temperature. Temperature (T) dependence of magnetic susceptibilities (χ) of $RbFeF_4$ and $CsFeF_4$ shows a typical two-dimensional antiferromagnetic behavior. On the other hand, in magnetic compound with S = 1, $CsVF_4$[12,13], a sharp $\chi(T)$ peak corresponding to an antiferromagnetic phase transition appeared at a magnetic field (H) of 200 Oe, and the $\chi(T)$ curves for field cooling (FC) and zero-field cooling (ZFC) overlapped. At $H \geq 5\,\mathrm{kOe}$, a ferromagnetic moment was induced by the magnetic field and the splitting of $\chi(T)$ curves for the FC and ZFC appeared. Therefore, we hope that mechanical stress can be used to switch the magnetic and/or ferroelectric domains in ferroelastic $A^{I}M^{III}F_4$ compounds.

Previously, we have intensively studied a series of chromium fluorides, $A^{I}CrF_4$ ($A^{I} =$ K and Cs), because of their highly frustrated magnetic structures such as triangular spin tubes[14,15]. Table 1 presents the structural phase diagram of $A^{I}CrF_4$ ($A^{I} =$ K, Rb, Cs), as previously reported by Kozak[16]. In equilateral triangular spin tube $CsCrF_4$, no structural isomer exists below the melting point. However, a structural isomer was observed in $KCrF_4$ and $RbCrF_4$ when the sintering temperature was varied. In $KCrF_4$, non-equilateral triangular spin tube α-$KCrF_4$ was crystallized below 768 °C [15], whereas β-$KCrF_4$ consisting of the $CsCrF_4$-type structure was crystallized above 768 °C. In $RbCrF_4$, α-$RbCrF_4$ consisting of a $TlAlF_4$-type structure was crystallized below 750 °C [17], whereas β-$RbCrF_4$, consisting of a $CsCrF_4$-type structure, is crystallized above 750 °C. The magnetic properties of $RbCrF_4$ were studied without any distinction between the α- and β-phases[18,19].

We have previously observed that the magnetic susceptibility of $CsCrF_4$ is strongly affected by a small amount of paramagnetic impurities and/or imperfect crystallization[14,15]. A crystallization method that enables the synthesis of high-quality α-$RbCrF_4$ must be developed to confirm the magnetic ground state. Figure 1 shows the aristotype structure of α-$RbCrF_4$, which we believe a quasi-two-dimensional Heisenberg antiferromagnet with S = 3/2. In this study, we obtained highly crystalline α-$RbCrF_4$ and performed X-ray diffraction (XRD) and magnetic susceptibility measurements to confirm that high-quality samples were prepared and to confirm the heretofore unreported magnetic properties of α-$RbCrF_4$.

Table 1: Structural phase diagram of $A^{I}CrF_4$ (A^{I} = K, Rb, and Cs) in Ref. 16.

	α - phase (low-T phase)	Critical Temperature (°C)	β - phase (high-T phase)
$KCrF_4$	non-equilateral triangular spin tube	768	$CsCrF_4$-type
$RbCrF_4$	square lattice ($TlAlF_4$-type)	750	$CsCrF_4$-type
$CsCrF_4$	equilateral triangular spin tube	No structural isomer below melting point.	

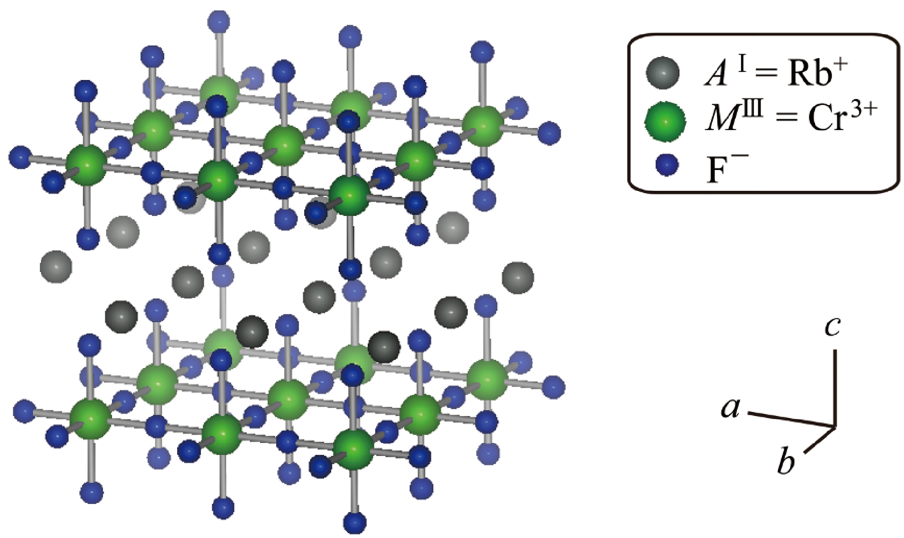

Figure 1: Schematic of aristotype structure of $A^{I}M^{III}F_4$ compound. Each layer is stacked without translation in the *ab*-plane. In α-$RbCrF_4$, A^{I} and M^{III} correspond to Rb^{+} and Cr^{3+}, respectively.

2. SAMPLE PREPARATION

We prepared polycrystalline samples of α-$RbCrF_4$ using a method similar to that employed in the synthesis of high-quality $CsCrF_4$, i.e., using a conventional solid-state reaction method[15]. We mixed the RbF and $CrF_3 \cdot 4H_2O$ starting materials in accordance with the stoichiometry and then heated them at 200 °C for more than 48 h under vacuum with $P < 1\times10^{-3}$ Pa to dehydrate the crystals. Sintering was then performed at various temperatures below 750 °C. The final sample color was dark green. To further purify the samples, we improved the pretreatment method before primary sintering, as discussed in the next section.

To examine the sample crystal structure and phase purity, we performed powder XRD measurements at room temperature. The XRD data were collected for $5° < 2\theta < 70°$ by a Philips X'pert Pro MPD using the Bragg-Brentano geometry with Cu $K\alpha$ radiation. Because the antiferromagnetic ground state in $CsVF_4$ was found to be broken by $H \geq 5\ \mathrm{kOe}$ [12,13], a weaker magnetic field should be applied to α-$RbCrF_4$. The temperature dependence of χ was measured using a superconducting quantum interference device magnetometer (Quantum Design, MPMS-XL) from 2 K to 350 K. In this study, we defined the magnetic susceptibility as $\chi \equiv M/H$. The FC and ZFC data were collected after applying H = 10 Oe and 1 kOe at T = 350 K and 2 K, respectively. Because the $\chi(T)$ curves for the FC and ZFC data overlapped, the ZFC data were omitted in the following discussion.

3. EXPERIMENTAL RESULTS AND DISCUSSION

Figure 2(a) presents the sharp XRD peak profiles obtained after sintering at 640 ℃. According to the previous studies, the space group of α-$RbCrF_4$ is *P*mmn ($2a \times 2b \times c$), and the lattice constants are $2a = 7.348$ Å and $c = 6.442$ Å [16,17,20]. On the basis of the *P*mmn ($2a \times 2b \times c$) space group, we can denote the all fundamental peaks using the indices shown in Fig. 2(a). However, additional XRD peaks appeared and their origin may be impurities and/or distorted square lattice caused by the tilting of CrF_6 octahedra. In $A^{\mathrm{I}}M^{\mathrm{III}}\mathrm{F}_4$, the *P*mmn ($2a \times 2b \times c$) space group is expected a ferroelastic state from Aizu's 4/mmm*Fmmm* notation.

We determined the best sintering temperature to be 640 ℃ and then post-annealed the samples at 500 ℃ under HF gas; we denote this as the usual method[15]. As shown in Fig. 2(b), we measured the T dependence of χ for α-$RbCrF_4$ at H = 10 Oe to prevent the saturation of impurity-induced weak ferromagnetic moments at high magnetic fields. As observed in $\chi(T)$ data for the samples obtained by the usual method, an anomaly indicating a weak ferromagnetic moment appeared at $T' = 15.0(5)\ \mathrm{K}$. As shown in Fig. 2(b), when we crystallized several samples under the same conditions, the transition temperatures T' remained unchanged; however, the values of χ at 2.0 K varied widely among different batches. We believe that this magnetic transition at T' is due to extrinsic properties, i.e., the presence of some magnetic impurities and/or poor crystallizations.

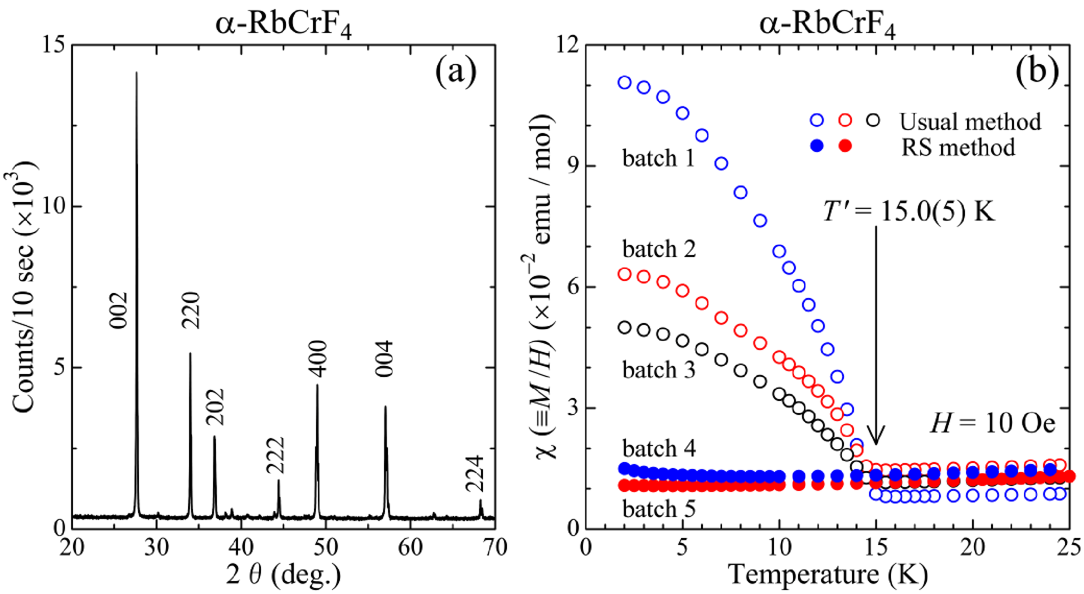

Figure 2: (a) X-ray diffraction pattern for α-$RbCrF_4$ after sintering at 640 °C. Fundamental peaks are denoted by the indices on the basis of the *Pmmn* ($2a \times 2b \times c$) space group. (b) Low-temperature magnetic susceptibility [$\chi(T)$] for samples obtained using the usual method in the three different batches (open circles) and the RS method in the two batches (closed circles). The all datasets agree with one another above $T'=15.0(5)$ K. However, an anomaly indicating the weak ferromagnetic moment appeared in the data for the samples obtained by the usual method, whereas no anomaly appeared in the data for the samples obtained by the RS method.

To further purify polycrystalline α-$RbCrF_4$, we improved the pretreatment of the sample before primary sintering at 640 °C. Figure 3 presents the scheme of the improved pretreatment, i.e., processes 3-6 were repeated several times before primary sintering. Finally, the samples were heated at 640 °C for 50 h under N_2 gas flow (200 cc/min) and then post-annealed at 500 °C under HF gas. We will denominate the improved pretreatment "the return to synthetic precursor method" (abbreviated as the RS method). As observed in Fig. 2(b), when we compare the data for the samples obtained using the RS method with those obtained using the usual method, the $\chi(T)$ curves for both methods agree with each other above 15 K; however, no anomaly appeared below 15 K in the data for the samples obtained by the RS method and its tendency showed high reproducibility. On the other hand, the weak ferromagnetic moment at 2.0 K for the samples using the usual method showed a large sample dependence. Therefore, we concluded that the impurity-induced weak ferromagnetic moments appeared in the samples using the usual method. Regretfully, the samples obtained by the two methods are indistinguishable based on the XRD data. In future, we will refine the superstructure for α-$RbCrF_4$ by another experimental methods such as EXAFS or XANFS experiment to obtain high-quality α-$RbCrF_4$ where the magnetic phase transition at T' will be absent.

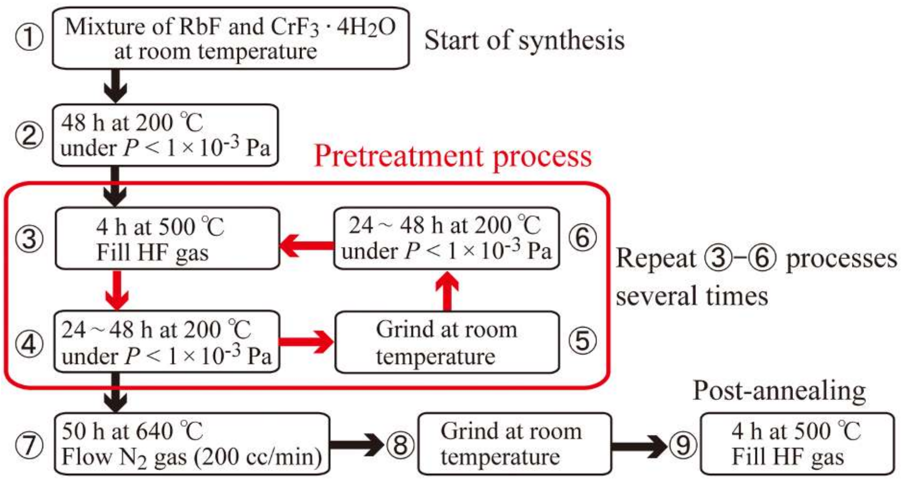

Figure 3: Schematic of the improved pretreatment for α-$RbCrF_4$. Processes 3-6 were repeated several times before primary sintering at 640 ℃. We will denominate the improved pretreatment "the return to synthetic precursor method" (abbreviated as the RS method).

Figure 4(a) shows the $\chi(T)$ curves at H = 1 kOe over the entire temperature range for the high-quality α-$RbCrF_4$. A broad $\chi(T)$ peak indicating a typical low-dimensional antiferromagnetic behavior appeared at $T_{\max} \approx 47\ \mathrm{K}$ [21]. As observed in the inset of Fig. 4(a), a sharp $\chi(T)$ peak appeared with the curvature similar to that of $CsVF_4$ at H = 200 Oe[12]. Therefore, we conclude that an antiferromagnetic phase transition occurs at T_N = 29.3(2) K in α-$RbCrF_4$. Figure 4(b) shows the 1/$\chi(T)$ curve. We fitted the 1/$\chi(T)$ data above 250 K to the Curie-Weiss law [$\chi(T) = C/(T - \Theta_{\mathrm{cw}})$ and $C = N_A g^2 \mu_B J(J+1)/(3k_B)$]; the resulting Weiss temperature (Θ_{cw}) and effective magnetic moment were $-67(3)\ \mathrm{K}$ and $3.98(3)\,\mu_B$, respectively. The effective magnetic moment agrees with the spin-only value $3.87(3)\,\mu_B$ within the experimental error. Applying the molecular field theory to solve the Hamiltonian given by

$$H_{\mathrm{cal}} = -2\sum_{\langle i,j \rangle} J_{i.j}\boldsymbol{S}_i \cdot \boldsymbol{S}_j\ , \qquad (3.1)$$

the Weiss temperature is written as

$$\Theta_{\mathrm{CW}} = \frac{2zJS(S+1)}{3k_B}, \qquad (3.2)$$

where z is the number of nearest neighbors and J is the isotropic exchange interaction, provided that this equation is valid for $T > |\Theta_{\mathrm{cw}}|$. Applying $\Theta_{\mathrm{cw}} = -67(3)\ \mathrm{K}$ and $z = 4$, we estimated the intra-layer exchange interaction to be $J_{\mathrm{intra}}/k_B = -6.7(3)\ \mathrm{K}$.

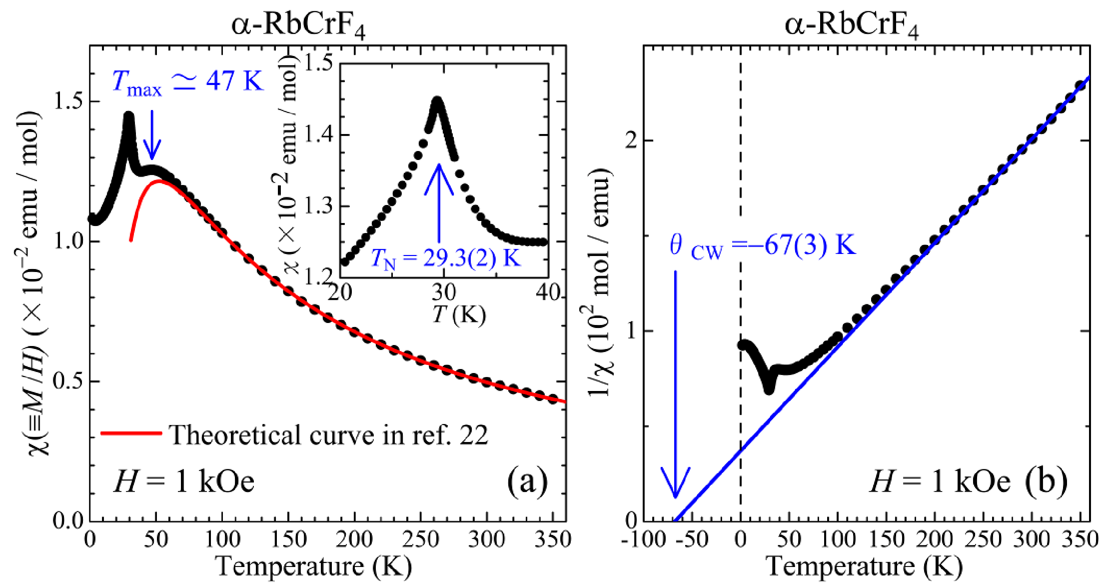

Figure 4: (a) Temperature dependence of the magnetic susceptibility (χ) for the high-quality α -RbCrF$_4$. A broad $\chi(T)$ peak appeared at $T_{\max} \approx 47$ K. The solid line is the best fit of the theoretical formula reported by Lines in Ref. 22, which yields $J_{\text{intra}} / k_{\text{B}} = -6.6$ K and $\chi_{\text{const}} = -9.4 \times 10^{-5}$ emu/mol. The inset shows a sharp peak for $\chi(T)$, indicating an antiferromagnetic phase transition at T_N = 29.3(2) K. (b) Temperature dependence of $1/\chi(T)$. The solid line is the Curie-Weiss law; the resulting Weiss temperature is $\Theta_{\text{CW}} = -67(3)$ K.

For a quadratic-layer Heisenberg antiferromagnet, the magnetic susceptibility reported by Lines can be expressed in the high-temperature region [$\chi_{2D}(T)$] by a series expansion[22]. To subtract the T-independent term (χ_{const}), i.e., the diamagnetic contribution and Van Vleck term, we attempted to use $[\chi_{2D}(T) + \chi_{\text{const}}]$ with the experimental data in the 200-350 K temperature range far above $|\Theta_{\text{CW}}|$. For the best-fit curve shown in Fig. 4(a), the values of J_{intra} and χ_{const} are determined to be $-6.6(1)$ K and $-9.4(1) \times 10^{-5}$ emu/mol, respectively. The values of J_{intra} obtained by the different analyses are in good agreement. Using the relation between J_{intra} and $T_{\max}$, we further obtained $J_{\text{intra}}/k_{\text{B}} = -T_{\max}/[1.12 \times S(S+1) + 0.10] = -5.5(2)$ K [22]. This value is smaller than the others. The broad $\chi(T)$ peak in α -RbCrF$_4$ is necessary to re-consider not only the development of an antiferromagnetic short-range order accompanied with the inter-layer exchange interaction (J_{inter}) but also the existence of the inequivalent magnetic sites, i.e., the tilting of CrF$_6$ octahedra in the opposite manner[20]. Based on the theoretical investigations of the effect of J_{inter} by Ginsberg, $\chi_{2D}(T)$ must be modified at $T < |\Theta_{\text{CW}}|$, but the value of $T_{\max}$ is almost invariant[23]. According to Yasudas' theoretical investigations of the relation between J_{inter} and T_N in both quantum and classical two-dimensional antiferromagnets, we obtained

$J_{\rm inter}/J_{\rm intra} \approx 0.05$ from Fig. 3 in Ref. 24, where we roughly estimated $(k_{\rm B}T_{\rm N})/[2|J_{\rm intra}|S(S+1)] \approx 0.6$. Based on the magnetic susceptibility and neutron diffraction experiments on $CsVF_4$, the magnetic ground state may change from the antiferromagnetic state to some other state with ferromagnetic moments at a critical magnetic field (H_c)[12,13]. In α-$RbCrF_4$, we re-expressed H_c at T = 0 K as $|g_1 - g_2|\mu_{\rm B}H_{\rm C} = 6|J_{\rm inter}|$, where g_1 and g_2 correspond to the g-value of each inequivalent magnetic site in antiferrodistortive CrF_6 octahedra[12]. Because $|g_1 - g_2| \approx 0.01-0.05$ in Cr^{3+} compounds[25], we roughly estimated the critical field as $H_{\rm C} \approx 2\times10^3 - 1\times10^4|J_{\rm inter}|/(g\mu_{\rm B})$. Consequently, we found that the $\chi(T)$ data at H =1 kOe shown in Fig. 4 indicate the presence of an intrinsic antiferromagnetic ground state. Thus, the absence of the differences between the FC and ZFC $\chi(T)$ curves is due to the absence of a ferromagnetic moment.

4. CONCLUSIONS

We successfully synthesized high-quality α-$RbCrF_4$, a quasi-two-dimensional Heisenberg antiferromagnet with S = 3/2 using the RS method, which is an improved pretreatment method. The RS method can be applied to many powdered polycrystalline or monocrystalline fluorides before primary sintering. XRD experiments revealed that α-$RbCrF_4$ consists of a $TlAlF_4$-type structure, which shows a good two-dimensionality. Magnetic susceptibility experiments did not find any extrinsic anomaly due to impurities at $T' = 15.0(5)$ K. The intrinsic $\chi(T)$ curve exhibited a broad $\chi(T)$ peak at $T_{\rm max} \approx 47$ K and showed the occurrence of an antiferromagnetic phase transition at $T_{\rm N}$ = 29.3(2) K. Using the $\chi(T)$ data in the high-T region, we obtained $J_{\rm intra}/k_{\rm B} = -6.6(1)$ K and $J_{\rm inter}/J_{\rm intra} \approx 0.05$. As a result, the $\chi(T)$ data at H =1 kOe indicate the presence of an intrinsic antiferromagnetic ground state. If the degree of the good two-dimensionality is increased, the antiferromagnetic ground state may change under low magnetic fields because of the competition between the Zeeman energy and $J_{\rm inter}$. We expect that the singular curvature of the $\chi(T)$ peak at $T_{\rm N}$ = 29.3 K is because of the existence of inequivalent magnetic sites, i.e., the different tilting schemes of the F^- octahedra surrounding the Cr^{3+} ions at different sites. In future, the superstructure will be determined to clarify whether ferromagneticity, ferroelectricity, and ferroelasticity coexist in this material. Furthermore, the temperature dependence of the heat capacity under high magnetic fields and high field magnetization process will be measured to confirm the magnetic-field-induced phase transition.

ACKNOWLEDGEMENTS

We are grateful to T. Goto, and T. Masuda for the stimulating discussions. We received valuable support from the Frontier Science Research Center in Kagoshima University for performing the powder XRD experiments. This research was partly supported by the Kurata Memorial Hitachi Science and Technology Foundation, and JSPS KAKENHI Grant Numbers JP22014009 and JP23684029.

COMPETING INTERESTS

The authors declare that no competing interests exist.

AUTHORS' CONTRIBUTIONS

All aspects of this work were carried out in close collaboration between both authors. Both authors read and approved the final manuscript.

REFERENCES

[1] Spaldin N. A., Cheong S. W., and Ramesh R. Multiferroics: Past, present, and future. Phys. Today 2010; 63: 38-43.

[2] Cheong S. W. and Mostovoy M. Multiferroics: a magnetic twist for ferroelectricity. Nat. Mater. 2007; 6: 13-20.

[3] Scott J. F. Data storage: Multiferroic memories. Nat Mater. 2007; 6: 256-257.

[4] Aizu K. Possible species of ferromagnetic, ferroelectric, and ferroelastic crystals. Phys. Rev. B 1970; 2: 754-772.

[5] Hagenmuller P. Inorganic Solid Fluorides: Chemistry And Physics Academic Press 1985.

[6] Kleemann W., Schfer F. J., and Nouet J. Structural phase transitions in ferroelastic $RbAlF_4$. II. Linear birefringence investigations. J. Phys. C: Solid State Phys. 1982; 15: 197-208.

[7] Bulou A. and Nouet J. Structural phase transitions in ferroelastic $TlAlF_4$: DSC investigations and structures determinations by neutron powder profile refinement. J. Phys. C: Solid State Phys. 1987; 20: 2885-2900.

[8] Abrahams S. C. and Bernstein J. L. Ferroelastic effect in $RbFeF_4$ and $CsFeF_4$. Mat. Res. Bull. 1972; 8: 715-720.

[9] Eibschutz M., Guggenheim H. J., and Holmes L. Magnetic behavior of a layer-type antiferromagnet $RbFeF_4$. J. Appl. Phys. 1971; 42: 1485-1486.

[10] Heger G. and Dachs H. Magnetic behavior of the two-dimensional antiferromagnet $RbFeF_4$. Solid State Commun. 1972; 10: 1299-1303.

[11] Eibschutz M., Guggenheim H. J., Holmes L., and Bernstein J. L. $CsFeF_4$: A new planar antiferromagnet. Solid State Commun. 1972; 11: 457-460.

[12] Ikeda H., Hidaka M., and Wanklyn B. M. Magnetic phase transition in $CsVF_4$. Physica B 1990; 160: 287-292.

[13] Hidaka M., Fujii H., Nishi M., and Wanklyn B. M. Magnetic Phase Transition in the Layer Compound $CsVF_4$. phys. stat. sol. (a) 1990; 117: 563-570.

[14] Manaka H., Hirai Y., Hachigo Y., Mitsunaga M., Ito M., and Terada N. Spin-liquid state study of equilateral triangle *S* = 3/2 spin tubes formed in $CsCrF_4$. J. Phys. Soc. Jpn. 2009; 78: 093701(1)-(4).

[15] Manaka H., Etoh T., Honda Y., Iwashita N., Ogata K., Terada N., Hisamatsu T., Ito M., Narumi Y., Kondo A., Kindo K., and Miura Y. Effects of geometrical spin frustration on triangular spin tubes formed in $CsCrF_4$ and α -$KCrF_4$. J. Phys. Soc. Jpn. 2011; 80: 084714(1)-(11).

[16] Kozak D. Rev. Chim. Miner. Etude de Quelques Composes Fluores du Chrome. 1971; t8: 301-337.

[17] Jorgensen C. K., Neilands J. B., Nyholm R. S., Reinen D., Williams R. J. P. editors. Structure and Bonding. Volume 3: Babel D. 1967; 3: 1-87.

[18] Knoke G. and Babel D. Z. Magnetic investigations of ternary chromium(III)-fluorides $ACrF_4$. Naturforschung B 1975; 30: 454-455.

[19] Kampe O., Frommen C., and Pebler J. Z. Magnetic studies of the compounds $ACrF_4$ (A=K, Rb, Cs) a Moessbauer study of ^{57}Fe-Doped $CsCrF_4$. Naturforschung. B 1993; 48: 1112-1120.

[20] Deblieck R., Tendeloo G. Van, Landuyt J. Van, and Amelinckx S. A structure cplassification of symmetry-related perovskite-like ABX_4 phases. Acta Cryst. 1985; B41: 319-329.

[21] Jongh L. J. de and Miedema A. R.: Experiments on simple magnetic model system: Adv. Phys. 1974; 23: 1-260.

[22] Lines M. E. The quadratic-layer antiferromagnet. J. Phys. Chem. Solids 1970; 3: 101-116.

[23] Ginsberg A. P. and Lines M. E. Magnetic exchange in transition metal complexes. VIII. Molecular field theory of intercluster interactions in transition metal cluster complexes. Inorg. Chem. 1972; 11: 2289-2290.

[24] Yasuda C., Todo S., Hukushima K., Alet F., Keller M., Troyer M., and Takayama H. Neel temperature of quasi-low-dimensional Heisenberg antiferromagnets. Phys. Rev. Lett. 2005; 94: 21720(1)-(4).

[25] Pake G. E. Paramagnetic Resonance: An Introductory Monograph: New York, W. A. Be3njamin 1962.